A Study on the Torsional Vibration Characteristics of Super Large Two Stroke Low Speed Engines with Tuning Damper

Ronald D Barro*·Sang Hwan Kim*·Don Chool Lee†

Key Words : *torsional vibration, tuning damper, two stroke low speed diesel engine*

ABSTRACT

Ship builder's requirement for a higher power output rating has lead to the development of super large two stroke low speed diesel engines. Usually a large-sized bore ranging from 8 - 14 cylinders, this engine group is capable of delivering power output of more than 100,000 bhp at maximum continuous rating. Other positive aspects of this engine type include higher thermal efficiency, reliability, durability and mobility. This all play a vital role in meeting the propulsion requirement of vessels, specifically for large container ships, of which speed is a primary concern to become more competitive. Consequently, this also resulted in the modification of engine parameters and new component designs to meet the consequential higher mean effective pressure and higher maximum combustion pressure. Even though the fundamental excitation mechanism unchanged, torsional vibration stresses in the propulsion shafting are subsequently perceived to be higher.

As such, one important viewpoint in the initial engine design is the resulting vibration characteristic expected to prevail on the propulsion shafting system (PSS). This paper investigated the torsional vibration characteristics of these super large engines. For the two node torsional vibration with a nodal point on the crankshaft, a tuning damper is necessary to reduce the torsional stresses on the crankshaft. Hence, the tuning torsional vibration damper design and compatibility to the shafting system was similarly reviewed and analyzed.

Nomenclatures

ω : Angular velocity
i : Number of lumped masses
m : Total number of cylinders
n : Total number of lumped masses
β_i : The i^{th} torsional angle
$\Delta\beta_i$: $\beta_i - \beta_{i+1}$
I_i : The i^{th} moment of inertia
k_i : Torsional stiffness of the i^{th} lumped mass
T_{io} : Excitation torque to each cylinder
α : Explosion phase angle of the i^{th} cylinder
$R(=I_d/I)$: Ratio of inertia moments
$\omega_0^2(=k/I)$: Natural angular frequency of the PSS
$\omega_d^2(=k_d/I_d)$: Natural angular frequency of the damper
$\lambda(=\omega/\omega_0)$: Ratio of excitation frequency to natural angular frequency of PSS
$\nu(=\omega_d/\omega_0)$: Ratio of damper natural angular frequency to PSS
$\theta_{st}(=T_0/k)$: Static angle displacement of the PSS
$c_c(=2I_d\omega_0)$: Critical damping coefficient
$\gamma(=c/c_c)$: Ratio of damping coefficients

† Mokpo National Maritime University
E-mail : ldcvib@mmu.ac.kr
Tel : (061) 240-7089, Fax : (061) 240-7282

* Mokpo National Maritime University
Graduate School-Department of Marine Engineering

1. Introduction

Two stroke low speed diesel engine has shown significant developments since its initial conception. From then, increased mean effective pressures and higher thermal efficiency has been the designer' s continued priorities. Some recent advancement affirmed the efforts with the introduction of engines capable of delivering power output above the 100,000 bhp mark.[1] These developments, however, also resulted in increased exciting torques and stresses resulting to several complicated vibration problems,

One of these vibration phenomena is the torsional vibration which demands a thorough understanding of its effect on the system. This vibration affects all rotating machinery and must be investigated thoroughly as it has a significant influence on the engine, hull and shafting system. Torsional analysis of the propulsion shafting system should be given considerations in the early design stage, thereby identifying the significant resonance conditions.[2] Torsional vibration is defined as the inertias' or rigid bodies' oscillations about the centre axis of the shaft line, or simply as the twist and its resonance caused by the explosion (gas) pressure and the inertia forces of cylinder and piston in reciprocating internal combustion engines.[3]

For the large-sized bore of 8~12, and 14 cylinders, the torsional vibration stresses and vibratory torque at the two node torsional vibration with a nodal point located at the crankshaft was emphasized.[4,5] Two twelve (12) cylinder engines with a 980 mm and 960 mm bore were employed as case study models. This study investigated the dynamic

characteristics of torsional vibrations of super large two stroke low speed engines with tuning damper. Onboard measurements were carried out to confirm the theoretical calculated value of the torsional vibration stresses of the PSS. Likewise, the angular velocities of the turning wheel were measured and the function of the Geislinger tuning damper was confirmed through its monitoring system.

2. Tuning damper basic theory for optimum design[6,7]

The ship' s propulsion shafting and damping system is actually regarded as a multi-degree of freedom system. However, it can be replaced by an equivalent inertia and stiffness forced vibration system, as can be seen in Figure 1, for calculation simplicity. For the case of damper design, an equivalent inertia moment I of the corresponding systems is $\sum_{i=1}^{n} I_i \beta_i^2$ and the equivalent stiffness k is $\sum_{i=1}^{n} k_i (\Delta \beta_i^2)$. The resultant vector of engine cylinder' s excitation torque is $\sum_{i=1}^{m} \beta_i T_{io} \cos(\omega t + \alpha)$, but for a two lumped mass system application when the phase lag is neglected it becomes $T_o \cos \omega t$.

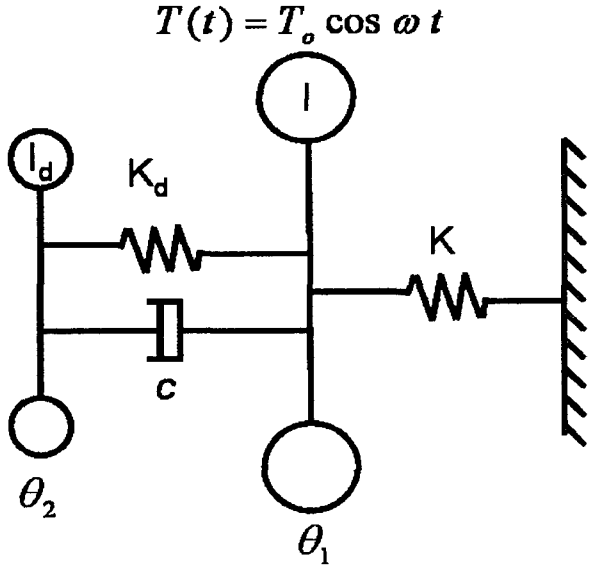

Figure 1 Two mass system model for torsional tuning damper

A resonance will occur in the damper if the natural angular frequency of main vibration system $\omega_n (\sqrt{k/I})$ is equal to the damper $\omega_d (\sqrt{k_d/I_d})$. It can be noted that for a system under free vibration conditions, that is without a exciting torque $T=0$, $\sum J\omega^2\theta = 0$ will be attained if ω is the natural frequency.[8]

When the damping coefficient of dash-pot c and the damper stiffness k_d and inertia mass moment I_d are attached to the main vibration system, and the corresponding angle amplitude are θ_1 and θ_2 respectively, then kinetic energy (T), elastic energy (U) and viscous energy (F) can be presented in the following equation:

$$2T = I\dot{\theta}_1^2 + I_d\dot{\theta}_2^2 \quad (1)$$

$$2U = k\theta_1^2 + k_d(\theta_2 - \theta_1)^2 \quad (2)$$

$$2F = c(\dot{\theta}_2 - \dot{\theta}_1)^2 \quad (3)$$

When excitation torque $T_o \cos \omega t$ is applied to an equivalent inertia moment I, the equations of motion of the two masses can be given as

$$I\ddot{\theta}_1 + k\theta_1 - k_d(\theta_2 - \theta_1) - c(\dot{\theta}_2 - \dot{\theta}_1) = T_o \cos\omega t \quad (4)$$

$$I_d\ddot{\theta}_2 + k_d(\theta_2 - \theta_1) + c(\dot{\theta}_2 - \dot{\theta}_1) = 0 \quad (5)$$

In order to solve the forced vibration problems, only the real part of the solution is considered and $\dot{\theta}_1, \ddot{\theta}_1, \dot{\theta}_2$, and $\ddot{\theta}_2$ will be obtained. The steady state solution of Equations (4) and (5) will be obtained as

$$\theta_1 = \mathrm{Re}\left[\frac{T_0 e^{i\omega t}\left[(k_d - I_d\omega^2) + i\omega c\right]}{\left[(k - I\omega^2)(k_d - I_d\omega^2) - I_d k_d\omega^2\right] + i\omega c(k - I\omega^2 - I_d\omega^2)}\right] \quad (6)$$

$$\theta_2 = \mathrm{Re}\left[\frac{T_0 e^{i\omega t}(k_d + i\omega c)}{\left[(k - I\omega^2)(k_d - I_d\omega^2) - I_d k_d\omega^2\right] + i\omega c(k - I\omega^2 - I_d\omega^2)}\right] \quad (7)$$

The absolute values of θ_1 and $\tan\delta_1$ in Equation (6) and (7) becomes

$$\theta_2 - \theta_1 = \mathrm{Re}\left[\frac{T_0 e^{i\omega t} I_d\omega^2}{\left[(k - I\omega^2)(k_d - I_d\omega^2) - I_d k_d\omega^2\right] + i\omega c(k - I\omega^2 - I_d\omega^2)}\right] \quad (8)$$

$$\theta_1 = \left[\frac{(k_d - I_d\omega^2)^2 + (\omega c)^2}{\left[(k - I\omega^2)(k_d - I_d\omega^2) - I_d k_d\omega^2\right]^2 + (\omega c)^2(k - I\omega^2 - I_d\omega^2)^2}\right]^{\frac{1}{2}} \times T_0 \cos(\omega t - \delta_1) \quad (9)$$

$$\tan\delta_1 = \left[\frac{\omega c(I_d\omega^2)^2}{\left[(k - I\omega^2)(k_d - I_d\omega^2) - I_d k_d\omega^2\right](k_d - I_d\omega^2) + (\omega c)^2(k - I\omega^2 - I_d\omega^2)}\right] \quad (10)$$

Equations (6) - (10) can be rearranged to Equations (11) to (16). Hence, the magnitudes, A_1 and A_2, can be expressed as

$$\theta_1/\theta_{st} = A_1\cos(\omega t - \delta_1)$$

$$A_1 = \left[\frac{(\nu^2 - \lambda^2)^2 + (2\gamma\lambda)^2}{(2\gamma\lambda)^2\{1 - (1+R)\lambda^2\}^2 + \{(1 - \lambda^2)(\nu^2 - \lambda^2) - R\nu^2\lambda^2\}^2}\right]^{1/2} \quad (11)$$

$$\delta_1 = \tan^{-1}\left[\frac{2\gamma\lambda(R\lambda^4)}{\{(1-\lambda^2)(\nu^2-\lambda^2)-R\nu^2\lambda^2\}(\nu^2-\lambda^2)+(2\gamma\lambda)^2\{1-(1+R)\lambda^2\}}\right] \quad (12)$$

$$\theta_2/\theta_{st} = A_2\cos(\omega t-\delta_2)$$

$$A_2 = \left[\frac{\nu^4+(2\gamma\lambda)^2}{(2\gamma\lambda)^2\{1-(1+R)\lambda^2\}^2+\{(1-\lambda^2)(\nu^2-\lambda^2)-R\nu^2\lambda^2\}^2}\right]^{1/2} \quad (13)$$

$$\delta_2 = \tan^{-1}\left[\frac{(2\gamma\lambda)\lambda^2(1-\lambda^2)}{\nu^2\{(1-\lambda^2)(\nu^2-\lambda^2)-R\nu^2\lambda^2\}+(2\gamma\lambda)^2\{1-(1+R)\lambda^2\}}\right] \quad (14)$$

Tuning dampers are usually employed for the purpose of enhancing the damping effect by enlarging the relative motion, that is, θ_{12} which is induced by resonance between damper and the main shafting systems. Hence,

$$(\theta_2-\theta_1)/\theta_{st} = A_{12}\cos(\omega t-\delta_{12})$$

$$A_{12} = \frac{\lambda^2}{\left[(2\gamma\lambda)^2\{1-(1+R)\lambda^2\}^2+\{(1-\lambda^2)(\nu^2-\lambda^2)-R\nu^2\lambda^2\}^2\right]^{1/2}} \quad (15)$$

$$\delta_{12} = \tan^{-1}\left[\frac{(2\gamma\lambda)\{1-(1+R)\lambda^2\}}{(1-\lambda^2)(\nu^2-\gamma^2)-R\nu^2\lambda^2}\right]^{1/2} \quad (16)$$

Equation (11) shows that the amplitude of vibration of the main system $\lambda = \omega/\omega_o$ is a function of R, ν, λ and γ.

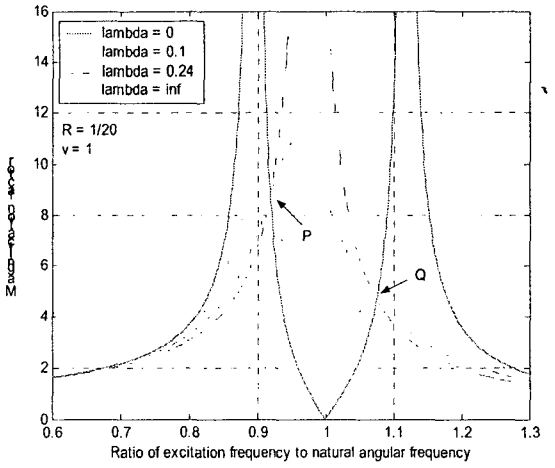

Figure 2 Effect of vibration damper on the vibratory system response

Figure 2 shows the graph of the variation in magnification factor A_1 for different damper damping coefficients and, where R=1/20 and the ratio of the natural frequency $\nu = 1$ are taken.

It will be noted that even if different damping coefficients of damper are given, the response curves will pass through a common point P and Q. The points P and Q can be located by substituting the extreme values of $\gamma = 0$ and $\gamma = \infty$ into Equation (11) to give:

$$(A_1)_{\gamma=0} = \frac{\nu^2-\lambda^2}{(1-\lambda^2)(\nu^2-\lambda^2)-R\nu^2\lambda^2} \quad (17)$$

$$(A_1)_{\gamma=\infty} = \frac{1}{1-(1+R)\lambda^2} \quad (18)$$

The optimum design criterion requires that the heights of P and Q be equal so that $(A_1)_{\gamma=0}(P) = -(A_1)_{\gamma=\infty}(Q)$. The negative sign on the Q point indicates the 180 degrees phase difference between P and Q points around the resonance condition. Hence, the resulting equation gives:

$$(2+R)\lambda^4 - 2\lambda^2(1+\nu^2+R\nu^2)+2\nu^2 = 0 \quad (19)$$

In addition, A_1 at P and Q points for $\gamma = \infty$ corresponds to Equation (18) from which Equation (20) can be obtained and is rearranged to give Equation (21).

$$\frac{1}{1-(1+R)\lambda_P^2} = -\frac{1}{1-(1+R)\lambda_Q^2} \quad (20)$$

$$\lambda_P^2+\lambda_Q^2 = \frac{2}{1+R} \quad (21)$$

$\lambda_P^2+\lambda_Q^2$ in Equation (21) is equivalent to the sum of two solutions of Equation (19) for λ^2 and Equation (22) can be derived.

$$\frac{2}{1+R} = \frac{2(1+\nu^2+R\nu^2)}{2+R} \quad (22)$$

Therefore, the condition of natural frequency ratio being equal at the same height of P and Q points corresponds to Equation (23). A damper which satisfies this condition can then be termed as a tuned vibration damper.[9]

$$\nu = \frac{1}{1+R} \quad (23)$$

However, Equation (23) does not indicate the optimal value of damping ratio γ and the corresponding value of A_1. As such, Equation (23) can be substituted into Equation (11). The condition of amplitudes of P and Q points being maximum values can be then calculated as follows:

$$\partial A_1/\partial\lambda = 0$$

$$\gamma_P^2 = \frac{R}{8(1+R)^3}\left(3-\sqrt{\frac{R}{2+R}}\right),\qquad \gamma_Q^2 = \frac{R}{8(1+R)^3}\left(3+\sqrt{\frac{R}{2+R}}\right) \quad (24)$$

Referring to Equation (23), the optimum ratio of the damping coefficients at P and Q

points takes different values but taking the average values will not cause much difference in the A_1 values. Hence the convenient optimal value of γ^2 can be given by Equation (25).

$$\gamma^2_{optimal} = \frac{3R}{8(1+R)^3} \tag{25}$$

For the optimal value of A_1, λ_P and λ_Q can be reduced using Equations (19) and (23) to give Equation (26). Thereby, A_1 becomes Equation (27).

$$\lambda_P^2, \lambda_Q^2 = \frac{1}{1+R} \pm \frac{1}{1+R}\sqrt{\frac{R}{2+R}} \tag{26}$$

$$|A_1|_{optimal} = \sqrt{1+\frac{2}{R}} \tag{27}$$

Furthermore, the principle of an actual ship design requires that the angular natural frequency of damper $\omega_d\left(\sqrt{K_d/I_d}\right)$ be slightly lower than ω_0 which corresponds to the natural frequency of main engine before dampers are installed. In this case, resonance will occur between inner and outer rings of the entire system and the relative angular velocity increases, thus the damping effect can be increased as well. Besides the optimum design criterion for dampers described previously, some other aspects of damper design also needs to be considered. This includes durability for which the damper spring member should be able to withstand the range of allowable vibration torque. Secondly, since the suggested allowable torsional vibration curves/values differs in each classification society, an economical design can be considered to suit its requirement. Lastly, the appropriate adjustment of P and Q points should also be paid with attention. Two adjusting methods can be done - i.e. adjusting the P point lower the Q point higher than the maximum continuous revolution while the other method is adjusting both P and Q points to be lower than the maximum continuous revolution. For the case of two node torsional vibration with one nodal point located on the crankshaft, it is recommended to locate the P and Q points at the same height following the torsional vibration allowable curve of the classification society.

3. Torsional vibration analysis and measurement of super large two stroke low speed engines

For the two node torsional vibration with nodal point located in the crankshaft, a damper is implemented in order to reduce the torsional vibration stresses. Similarly, a damper is necessary if resonance occurs around the maximum continuous revolution and a barred operation zone (critical speed) can not be assigned. For the purpose of this study, a 12K98MC and a 12RT-flex 96C-B engine were used as case models. Likewise, with the damping coefficient becoming larger in the second node vibration than the one node vibration system, a Geislinger type damper was installed to control the second node vibration.
In a multi-lumped mass system, the propeller, engine and damper will show complex dynamic behaviours. On the other hand, in the actual design process, damper size, stiffness, and optimum damping coefficient are evaluated, and the damper and shafting torsional vibration torque can then be calculated and kept within the manufacturer' s acceptable levels.

For the two node vibration, the excitation order to be considered is higher than that of a one node vibration. Thus the excitation force (harmonic coefficient) inducing the actual torsional vibration is smaller and the nodal point will be located on the crankshaft. Equally, the equivalent mass of the engine is smaller when compared to the one node vibration system as well as the torsional angle of the propeller. Therefore the effect of the equivalent mass of the propeller on the equivalent mass of the propulsion shaft is negligible. Lastly, the phase vector of the excitation force is not equal and for this reason, vibration can be controlled by a relatively small damper compared to the engine size.

Torsional vibration stresses and angular velocities were measured at the intermediate shaft and turning wheel to confirm the torsional stresses of the PSS and the function of the Geislinger tuning damper. The torsional vibration stress measurement was acquired on both the normal firing condition and one cylinder misfiring condition of the engine. A tele-metering system was installed at the intermediate shaft for the measurement of the torsional vibration stresses. The angular velocity was measured by Onosokki F-V converter 1300 and the gap sensor AEC PU-30 which was installed close to the turning wheel. Signal outputs were stored in a Sony 208A tape recorder while the FFT analyzer DI 2200 was used to analyze the acquired data.

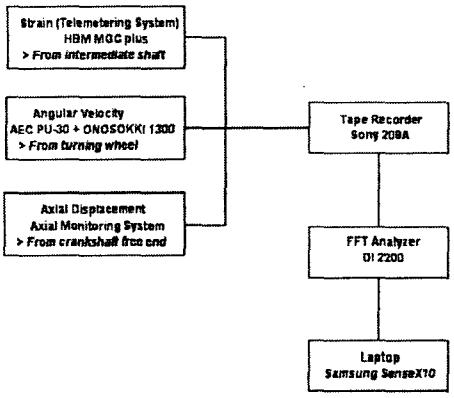

Figure 3 Schematic diagram for torsional vibration measurement

3.1 12K98MC-Mk6 engine with chain drive

Table 1 Specification for 12K98MC-Mk6

Engine	Type	12K98MC Mk6
	Max. Continuous output	93,360 bhp
	Max. Continuous speed	94.0 rpm
	Cylinder bore	980.0 mm
	Stroke	2660.0 mm
	Number of cylinder	12
	Mean indicated pressure	19.5 bar
	Ratio of connecting rod	0.413
	Reciprocating mass	18149 kg/cyl
	Firing Order	1-8-12-4-2-9-10-5-3-7-11-6
Damper	Type	Geislinger D280/11
	Inner Inertia	1410 kgm^2
	Outer Inertia	13000 kgm^2
	Torsional Stiffness	68 MNm/rad
	Damping	300 kN-m · s/rad
	Permissible Elastic Torque	703 kNm
	Permissible Damping Torque	101 kNm/bar
	Permissible Thermal Load	200 Kw
	Required Oil Quantity	220 liter/min
Propeller	Type	FPP
	Moment of Inertia in water	0.6385E+06 kgm^2 (mr^2)
	Number of blades	6
	Diameter	9100 mm
	Weight	105 ton

Table 2 Natural frequencies calculation [10]

Node	Calculated Value (CPM)	Measured Value (CPM)
1	164.92	About 165 (5.2 Hz)
2	628.71	About 660-670(11.1Hz)
3	765.94	About 740 (12.3 Hz)

As previously stated in this paper, torsional vibration stresses for the super large two stroke low speed diesel engine are said to exist and to be higher on the two node torsional vibration with a nodal point located in the crankshaft. The schematic diagram of mass system for 12K98MC engine is shown in Figure 4.

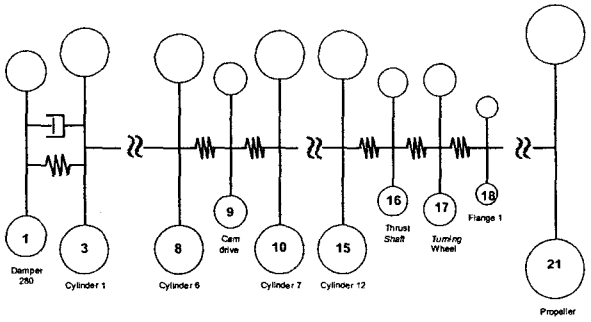

Figure 4 Schematic diagram of mass system for 12K98MC engine

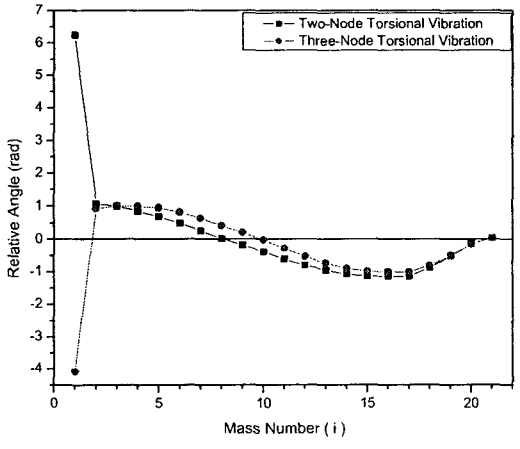

Figure 5 Mode shapes of torsional vibrations for 12K98MC engine

Figure 5 represents the vibration mode of second and third node torsional vibration. It indicates the torsional stress of crankshaft for the 12K98MC engine, a nodal point at two node torsional vibrations is located between cylinder No. 6 and the chain drive. The

calculated natural frequency at the two node torsional vibration of the PSS is 73.61rad/s before the damper was installed. Equivalent inertia moment and stiffness were also calculated as 317,428 kgm^2 and 173 MN-m/rad. The ratio of inertia moments (I_d / I) is about R=1/25.

Figure 6 shows the calculation of torsional stresses of the PSS and the system' s response with the damper installed. The calculated torsional stresses were 8.5N/mm^2 at 73RPM and 39N/mm^2 at 78RPM with damper and without damper respectively.

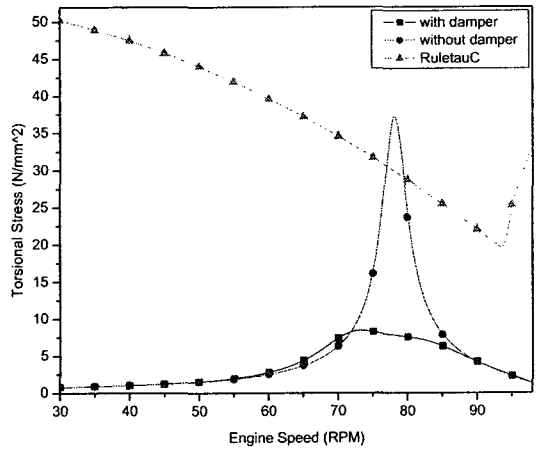

Figure 6 Torsional vibration stress of crankshaft for the 12K98MC engine

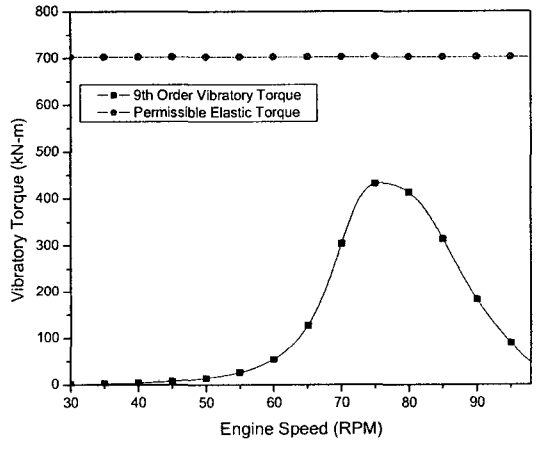

Figure 7 Vibratory torque of D280/11 damper for 12K98MC engine

Figure 7 illustrates the Damper D280/11 design for permissible elastic torque which is 703kN-m. The vibratory torque at the 9^{th} order was measured to be around 430kN-m.

Figures 8 and 9 compare the theoretical and measured angular velocities at the outer and inner damper. At Figure 8, theoretical data indicated the damper' s angular velocity peak value at 74 RPM to be 468mrad/sec. However, actual measurements revealed higher angular velocities value at the outer damper nearing the engine' s MCR. At 84RPM, the calculated outer damper angular velocity indicates a reducing slope whereas the measured angular velocity had a little change in its value. A difference can be seen at the engine' s MCR of 98RPM wherein the calculated and measured angular velocity were established at around 125 and 280mrad/sec and this condition within this range may be attributed to measurement errors at the Geislinger damper monitoring system.

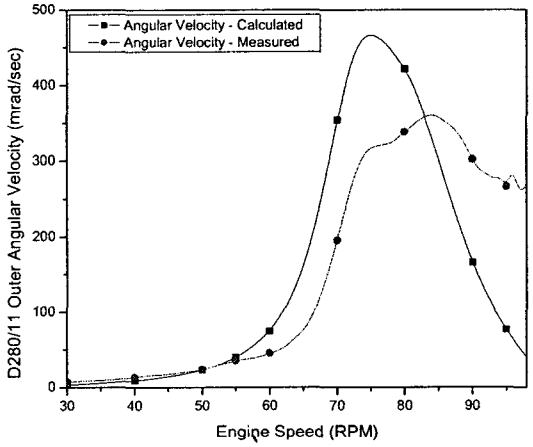

Figure 8 The 9^{th} order angular velocity of outer damper for 12K98MC engine

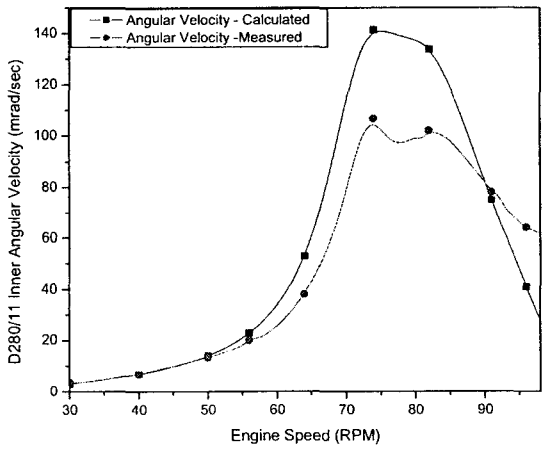

Figure 9 The 9^{th} order angular velocity of inner damper for 12K98MC engine

For the inner angular velocity, Figure 9 indicates the same pattern with that of the outer angular velocity. The measured and

calculated values were confirmed at around 106mrad/sec and 141mrad/sec respectively at MCR.

The 9th order torsional vibration stress of the intermediate shaft is seen on Figure 10. The calculated torsional stress is around 1.5N/mm^2. Measured values, however, indicated the torsional stress at 1.1N/mm2 at resonance peak 74 RPM.

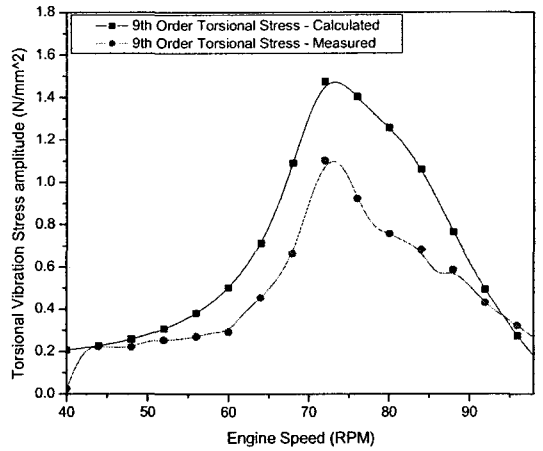

Figure 10 The 9th order torsional vibration stress of intermediate shaft for 12K98MC engine

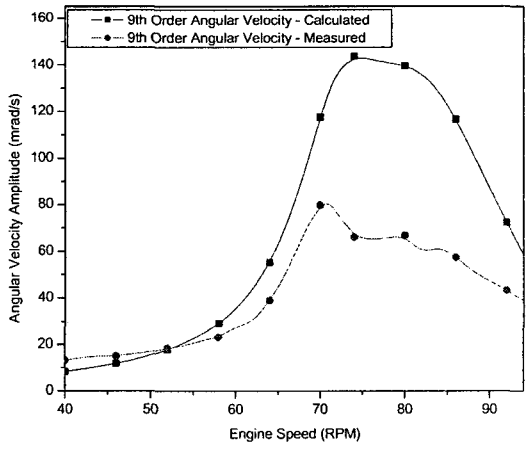

Figure 11 The 9th order angular velocity of turning wheel for 12K98MC engine

The 9th order angular velocity of the turning wheel was measured to be 82mrad/s at a resonance peak of 74 RPM (Figure 11) compared to the calculated value of 141mrad/s.

3.2 12RT-flex 96C-B engine with gear drive

A 12RT-flex 96C-B engine having a shaft power of around 93,360 SHP at 102RPM was used as the second study model and emphasis was likewise focused on the two node torsional vibration of the PSS.

Table 3 Specification for 12RT-flex96C-B Engine

Engine	Type	12RT-flex 96C-B
	Max. Continuous output	93,360.0 bhp
	Max. Continuous speed	102.0 rpm
	Cylinder bore	960.0 mm
	Stroke	2500.0 mm
	Number of cylinder	12
	Mean indicated pressure	19.89 bar
	Ratio of connecting rod	0.434
	Reciprocating mass	17834.0 kg/cyl
	Firing Order	1-9-11-4-3-8-10-6-2-7-12-5
Damper	Type	Geislinger D260/28
	Inner Inertia	540 kgm^2
	Outer Inertia	9760 kgm^2
	Torsional Stiffness	57 MNm/rad
	Relative Damping Coefficient	240 kN-m · s/rad
	Permissible Elastic Torque	653 kNm
	Permissible Thermal Load	160 kW
	Oil Flow	160 liter/min
Propeller	Type	FPP
	Moment of Inertia in air	0.310E+06 kgm^2
	Moment of Inertia in water	0.422E+06 kgm^2
	Number of blades	6
	Diameter	9700 mm

Table 4 Natural frequencies calculation [11]

Node	Calculated Value (CPM)	Measured Value (CPM)
1	196.81 (3.28 Hz)	About 196(3.27 Hz)
2	652.94 (10.88 Hz)	About 684(11.4 Hz)
3	790.84 (13.18 Hz)	About 780(13.0 Hz)

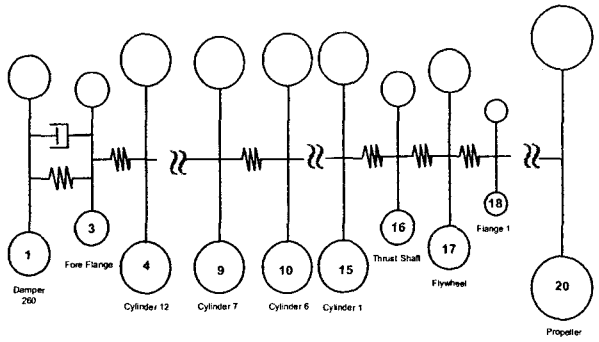

Figure 12 Schematic diagram of mass system for 12RT-flex 96C-B engine

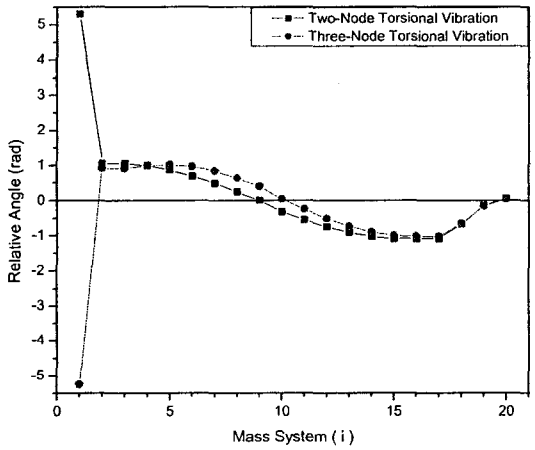

Figure 13 Mode shapes of torsional vibrations for 12RT-flex 96C-B engine

From Figure 13, the two node torsional vibration calculation located one nodal point between engine cylinder number 7 and cylinder number 6. The natural frequency before the damper was installed is 74.73rad/s. Equivalent inertia moment and stiffness were also calculated as 283,708 kgm^2 and 159 MN-m/rad. The ratio of inertia moments (I_d / I) is about R=1/30.

Figure 14 shows the calculated torsional stresses to be 35N/mm^2 at 78RPM and 7.8N/mm^2 at 73RPM for without damper and with damper system respectively. In addition, it can be seen that for the undamped mass system, the torsional stress limit was barely exceeded. Hence, the use of a smaller damper size can be employed.

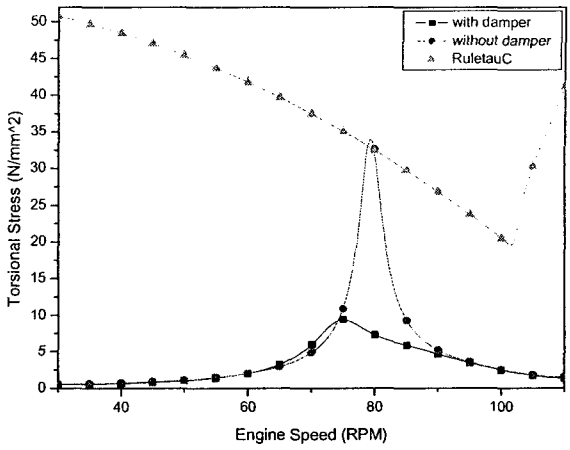

Figure 14 Torsional vibration stress of crankshaft for the 12RT-flex 96C-B engine

Figure 15 shows the vibratory torque at the 9^{th} order to be around 357kN-m at 76 RPM and the 653kN-m permissible elastic torque limit.

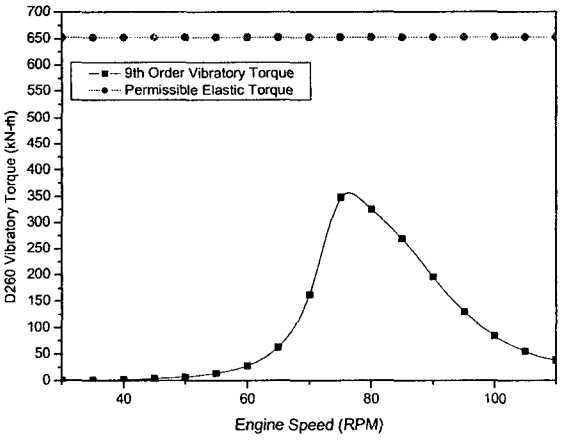

Figure 15 Vibratory torque of D260/28 damper for 12RT-flex 96C-B engine

Figure 16 and 17 shows the behaviour of the RT-flex engine' s inner and outer damper. On Figure 16, the outer damper peak resonance at 76 RPM has an angular velocity of 511mrad/s for its calculated value while the actual measurements revealed the peak value to be around 400mrad/s at 81 RPM. A noticeable deviation on the outer damper angular velocity nearing the MCR can be attributed again to measuring errors. Yet again, the measured data is evidently higher than the theoretical calculation.

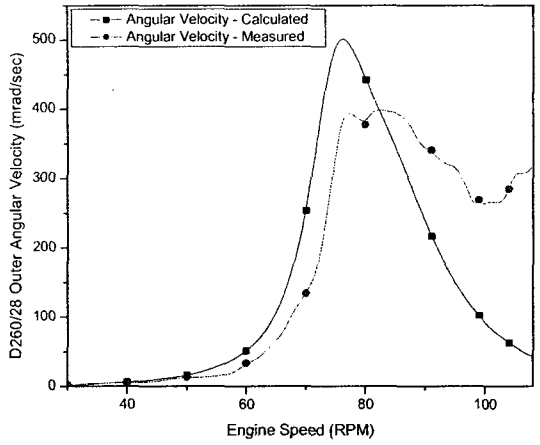

Figure 16 The 9th order angular velocity of outer damper for 12RT-flex 96C-B engine

For the inner damper, it exhibited a near identical value for the measured and calculated angular velocity (Figure 17). The peak amplitude at 76RPM shows a 159mrad/s and 165mrad/s angular velocity with the measured value a bit higher. Consequently, the calculated and measured angular velocity at MCR (102RPM) is 50mrad/s and 66mrad/s

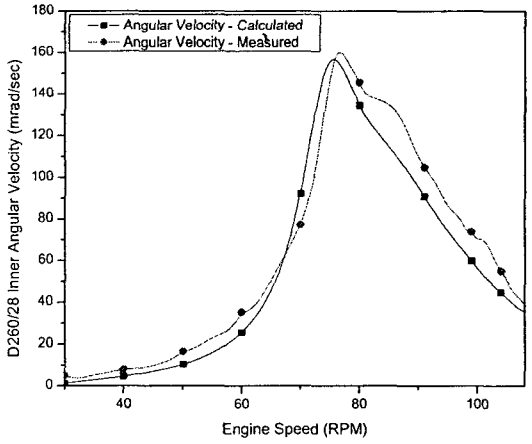

Figure 17 The 9th order angular velocity of inner damper for 12RT-flex 96C-B engine

The 9th order torsional vibration stress of the intermediate shaft was measured to be 1.8 N/mm^2 at a resonance peak of 75 RPM (Figure 18). Additionally, the 9th order angular velocity of the fly wheel was measured to be 135mrad/s at a resonance peak of 74 RPM (Figure 19) compared to the calculated value of 160mrad/s.

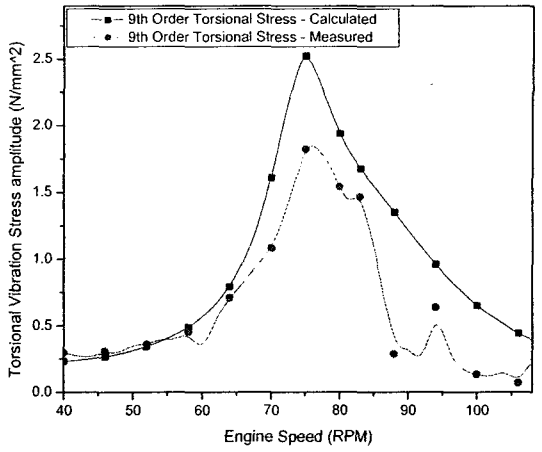

Figure 18 The 9th order torsional vibration stress of intermediate shaft for 12RT-flex 96C-B

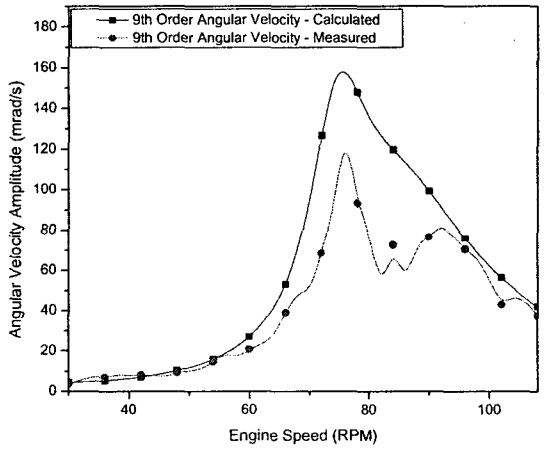

Figure 19 The 9th order angular velocity of flywheel for 12RT-flex 96C-B

4. Conclusion

For super large two stroke low speed diesel engines, the significant resonances and torsional stresses were exhibited at the 9th order of the two node torsional vibration with a nodal point located at the crankshaft of 12K98MC and 12RT-flex 96C-B. Hence, a tuning torsional vibration damper was designed and installed in these engines and investigated the dynamic characteristis of torsional vibration. The results are summarized as follows:

1. For optimum tuning damper design, the multi-lumped mass system can be substituted with a two mass system for

theoretical calculation. This method can be applied conveniently to tuning damper design.

2. Four torsional vibration measuring points of the 12K98MC and 12RT-flex 96C-B engines were compared and evaluated. The calculated and measured torsional stresses of the crankshaft and intermediate shaft, and the outer damper angular velocity of both engines have shown proportional pattern. For 12K98MC engine with chaindrive and 12RT-flex 96C-B with gear drive, theoretical calculation of torsional vibration stresses at the crankshaft were reduced by 80 percent with the damper employed. In addition, measured torsional stresses and outer damper angular velocities is about 70 per cent of the theoretical calculations. Hence, the actual response of the PSS and the damping system can be predicted and referred for new designs.
3. The vibration monitoring system of angular velocities at inner and outer has shown inaccuracies on the measurement values. Hence the data provided by the vibration monitoring system can check the damper function but will not provide precise data for the torsional vibration analysis of the propulsion shafting system.
4. The dynamic response of 12RT-flex 96C-B engine' s calculated and measured inner damper angular velocities was found to be almost equal, though this can not be attributed solely on measurement errors, this circumstance necessitates further study.

Reference

(1) MAN B&W Diesel, 2006, First MAN B&W Diesel Engine Over 100000 BHP Now In Service, Press Release.

(2) Det Norske Veritas, Cost-Saving Vibration Calculation for Shafting Systems, DNV.

(3) Lee, D.C, et al, 1992, A Study on the Dynamic Characteristics and Performance of Geislinger Type Torsional Vibration Damper for Two stroke Low Speed Diesel Engines, Journal of the Korean Society of Marine Engineering, Vol 16 No 5, pp 329-340.

(4) MAN B&W, 1988, Vibration Characteristics of Two Stroke Low Speed Diesel Engines, MAN B&W.

(5) MAN B&W, 2000, An Introduction to Vibration Aspects of Two Stroke Diesel in Ships, MAN B&W.

(6) Hyundai Heavy Industries Co. Ltd., Dynamic Characteristics and Performance of Tuning Torsional Vibration Damper for Hyundai – MAN B&W Two Stroke Low Speed Diesel Engine, MAN B&W Diesel AS, Meeting of Licensees, 1993.

(7) Nestorides, EJ, 1958, A Handbook on Torsional Vibration, BICERA Research Laboratory, Cambridge University Press.

(8) Wachel, JC, Szenazi, FR, 1993, Analysis of Torsional Vibrations in Rotating Machinery, 22nd TurboMachinery Symposium.

(9) Rao, Singiresu S, 2004, Mechanical Vibrations – Fourth Edition, Pearson – Prentice Hall.

(10) Dynamics Laboratory of MMU, 2006, Technical Report (Torsional Vibration Measurement for Hyundai-Samho Ship), Document No. MDL-06051.

(11) Dynamics Laboratory of MMU, 2006, Technical Report (Torsional Vibration Measurement for Hyundai-Samho Ship), Document No. MDL-06101.